Inorg. Chem. **2009**, *48*, 4295−4305

Alteration of Molecular Conformations, Coordination Modes, and Architectures for a Novel 3,8-Diimidazol-1,10-phenanthroline Compound in the Construction of Cadmium(II) and Zinc(II) Homochiral Coordination Polymers Involving an Auxiliary Chiral Camphorate Ligand

Li Wang, Wei You, Wei Huang,* Cheng Wang, and Xiao-Zeng You

State Key Laboratory of Coordination Chemistry, Nanjing National Laboratory of Microstructures, School of Chemistry and Chemical Engineering, Nanjing University, Nanjing 210093, P. R. China

Received December 25, 2008

A novel 3,8-diimidazol-1,10-phen (phen = phenanthroline) compound has been prepared from the carbon−nitrogen bond cross-coupling reaction. X-ray structural studies for this compound and its dihydrate reveal they have different molecular conformations (L_b in **1** and $L_c \cdot 2H_2O$ in **2**). Two cadmium(II) and one zinc(II) complexes of 3,8-diimidazol-1,10-phen, formulated as $[Cd_2(D\text{-cam})_2(L_a)_2] \cdot (H_2O)_6$ (**3**), $[Cd_2(D\text{-cam})_2(L_a)(H_2O)]$ (**4**), and $[Zn_2(D\text{-cam})_2(L_b)_2] \cdot (H_2O)_5$ (**5**), have been obtained involving an auxiliary chiral ligand D-cam (a dianion of D-camphoric acid) where the 3,8-diimidazol-1,10-phen ligand shows different molecular conformations, coordination modes, and architectures. Furthermore, D-cam and 3,8-diimidazol-1,10-phen ligands exhibit different bridging fashions to construct a homochiral 2D coordination polymer **3** and two homochiral 3D coordination polymers **4** and **5**. Density function theory computational studies on comparing the different molecular conformations of the 3,8-diimidazol-1,10-phen ligand as well as spectral, nonlinear optical, and thermal properties for related compounds before and after the metal-ion complexation have also been carried out.

Introduction

Recently, the research interest on coordination polymers and porous metal-organic frameworks is rapidly increasing because of their aesthetic architectures and fascinating potential applications on gas adsorption, ion exchange, catalysis, photoluminescence, electric conductivity, and so on.[1−5] Preparation of these coordination polymers is always based on many factors, especially the metal ions and counterions with different charge, size, and geometrical requirements for coordination as well as the number of coordination sites of organic building blocks. Metal complexes of 1,10-phen and its derivatives often show attractive chemical and physical properties in the area of coordination chemistry, material chemistry, analytical chemistry, metalloenzymes, probes of nucleic acids, and redox processes because of their strong chelating abilities and good π-conjugated character of ligands.[6] To date, many metal complexes

* To whom correspondence should be addressed. E-mail: whuang@nju.edu.cn.

(1) (a) Kitagawa, S.; Uemura, K. *Chem. Soc. Rev.* **2005**, *34*, 109. (b) Kesanli, B.; Lin, W. *Coord. Chem. Rev.* **2003**, *246*, 305. (c) Rao, C. N. R.; Natarajan, S.; Vaidhyanathan, R. *Angew. Chem., Int. Ed.* **2004**, *43*, 1466. (d) Pan, L.; Olson, D. H.; Ciemnolonski, L. R.; Heddy, R.; Li, J. *Angew. Chem., Int. Ed.* **2006**, *45*, 616.

(2) (a) Batten, S. R.; Robson, R. *Angew. Chem., Int. Ed.* **1998**, *37*, 1460. (b) Kitagawa, S.; Kitaura, R.; Noro, S. I. *Angew. Chem., Int. Ed.* **2004**, *43*, 2334. (c) Robin, A. Y.; Fromm, K. M. *Coord. Chem. Rev.* **2006**, *250*, 2127. (d) Dalgarno, S. J.; Thallapally, P. K.; Barbour, L. J.; Atwood, J. L. *Chem. Soc. Rev.* **2007**, *36*, 236.

(3) (a) Yaghi, O. M.; O'Keeffe, M.; Ockwig, N. W.; Chae, H. K.; Eddaoudi, M.; Kim, J. *Nature (London)* **2003**, *423*, 705. (b) Janiak, C. *Dalton Trans.* **2003**, 2781. (c) Eddaoudi, M.; Moler, D. B.; Li, H.; Chen, B.; Reineke, T. M.; O'Keeffe, M.; Yaghi, O. M. *Acc. Chem. Res.* **2001**, *34*, 319.

(4) (a) Férey, G.; Mellot-Draznieks, C.; Serre, C.; Millange, F.; Dutour, J.; Surblé, S.; Margiolaki, I. *Science* **2005**, *309*, 2040. (b) Zhao, X.; Xiao, B.; Fletcher, A. J.; Thomas, K. M.; Bradshaw, D.; Rosseinsky, M. J. *Science* **2004**, *306*, 1012. (c) Hagrman, P. J.; Hagrman, D.; Zubieta, J. *Angew. Chem., Int. Ed.* **1999**, *38*, 2639.

(5) (a) Halder, G. J.; Kepert, C. J.; Moubaraki, B.; Murray, K. S.; Cashion, J. D. *Science* **2002**, *298*, 1762. (b) Evans, O. R.; Ngo, H. L.; Lin, W. *J. Am. Chem. Soc.* **2001**, *123*, 10395. (c) Fang, Q. R.; Zhu, G. S.; Xue, M.; Sun, J. Y.; Tian, G.; Wu, G.; Qiu, S. L. *Dalton Trans.* **2004**, 2202. (d) Fang, Q. R.; Zhu, G. S.; Xue, M.; Sun, J. Y.; Wei, Y.; Qiu, S. L.; Xu, R. R. *Angew. Chem., Int. Ed.* **2005**, *44*, 3845.

(6) (a) Schilt, A. *Applications of 1,10-Phenanthroline and Related Compounds*; Pergamon: London, 1969. (b) Tomasik, P.; Ratajewicz, Z. *Pyridine Metal Complexes*; John Wiley & Sons: New York, 1985. (c) Sammes, P. G. ; Yahioglu, G. *Chem. Soc. Rev.* **1994**, *23*, 327. (d) Chelucci, G.; Thummel, R. P. *Chem. Rev.* **2002**, *102*, 3129.

10.1021/ic802445q CCC: $40.75
Published on Web 04/07/2009

bearing substituent 1,10-phen ligands have been prepared and characterized.[7−12] However, there are only several structural investigations on 3,8 substituted 1,10-phen compounds.[13−15]

In our previous work, 3,8-bis(4-mercaptophenyl)-1,10-phen, 3,8-bis(3′,4′-dibutyl-5″-mercapto-2,2′:5′,2″-terthiophen-5-yl)-1,10-phen and their respective Ru(II) complexes were prepared and used to combine with active gold nanoparticles on 1 μm gap gold electrodes in order to prepare photoresponsive self-assembled nanocomposite thin films.[14,15] Both of the above-mentioned 3,8-thiophene- and 3,8-phenyl-substituted 1,10-phen semiconductor compounds were prepared by the carbon−carbon bond cross-coupling reaction. As for the carbon−nitrogen bond cross-coupling reaction of 3,8-dibromo-1,10-phen, only one example of palladium(II)-catalyzed diarylamino-1,10-phen derivatives was reported.[16] In this work, we focus on synthesizing a new multidentate ligand 3,8-diimidazol-1,10-phen via the carbon−nitrogen bond cross-coupling reaction between 3,8-dibromo-1,10-phenanthroline and imidazole using Ullmann condensation methods[17] because this ligand has the following structural characters: (i) It has a more delocalized π-system than 1,10-phen, which will facilitate the transportation of electron within the molecule. (ii) The stereochemistry and conformation of this ligand (trans/trans, trans/cis, and cis/cis) are interesting in the formation hydrogen contacts and coordinative bonds because of the free rotation of the C−N single bonds between the two side imidazole rings and the central phen ring (Scheme 1). (iii) The number of the possible coordination sites is variable and diverse coordination modes, architectures, and topologies, such as helical and zigzag structures in this work, can be expected under different experimental conditions by using this imidazole-terminated phen bridging ligand.

Scheme 1. Schematic Illustration of Isomers of 3,8-Diimidazol-1,10-phen Ligand in Different Conformations

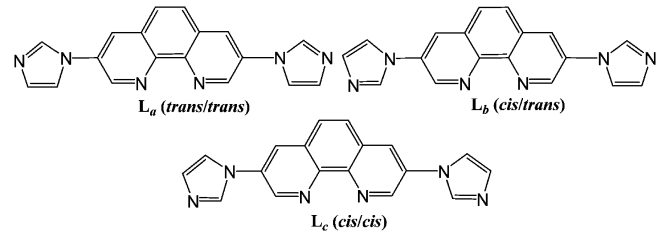

In view of the aforementioned structural characters of 3,8-diimidazol-1,10-phen, it is possible for us to construct certain chiral coordination polymers by inducing some chiral sources, which may have potential applications in the area of asymmetric catalysis, enantioselective separation, ion exchange, proton conductivity, intercalation chemistry, photochemistry and material chemistry.[18] In this paper, we use an extensively studied D-camphoric acid (D-H_2cam) as an auxiliary ligand[19,20] and report one 2D $[Cd_2(D\text{-}cam)_2(L_a)_2]\cdot(H_2O)_6$ (**3**) and two 3D homochiral coordination polymers $[Cd_2(D\text{-}cam)_2(L_a)(H_2O)]$ (**4**) and $[Zn_2(D\text{-}cam)_2(L_b)_2]\cdot(H_2O)_5$ (**5**) (Scheme 2), together with 3,8-

(7) (a) Zong, R. F; Thummel, R. P. *J. Am. Chem. Soc.* **2004**, *126*, 10800. (b) Muniz, K.; Nieger, M. *Angew. Chem., Int. Ed.* **2006**, *45*, 2305. (c) Stahl, S. S.; Thorman, J. L.; Nelson, R. C.; Kozee, M. A. *J. Am. Chem. Soc.* **2001**, *123*, 7188. (d) Hitchcock, P. B.; Hulkes, A. G.; Lappert, M. F.; Li, Z. N. *Dalton Trans.* **2004**, 129.

(8) (a) Dhar, S.; Senapati, D.; Das, P. K.; Chattopadhyay, P.; Nethaji, M.; Chakravarty, A. R. *J. Am. Chem. Soc.* **2003**, *125*, 12118. (b) Seebacher, J.; Ji, M.; Vahrenkamp, H. *Eur. J. Inorg. Chem.* **2004**, 409. (c) Fanizzi, F. P.; Margiotta, N.; Lanfranchi, M.; Tiripicchio, A.; Pacchioni, G.; Natile, G. *Eur. J. Inorg. Chem.* **2004**, 1705. (d) Berlinguette, C. P.; Dragulescu-Andrasi, A.; Sieber, A.; Galan-Mascaros, J. R.; Gudel, H. U.; Achim, C.; Dunbar, K. R. *J. Am. Chem. Soc.* **2004**, *126*, 6222. (e) Berlinguette, C. P.; Dragulescu-Andrasi, A; Sieber, A.; Gudel, H. U; Achim, C.; Dunbar, K. R. *J. Am. Chem. Soc.* **2005**, *127*, 6766.

(9) (a) Miller, M. T.; Gantzel, P. K.; Karpishin, T. B. *J. Am. Chem. Soc.* **1999**, *121*, 4292. (b) Hoffmann, S. K.; Corvan, P. J.; Singh, P.; Sethulekshmi, C. N.; Metzger, R. M.; Hatfield, W. E. *J. Am. Chem. Soc.* **1983**, *105*, 4608. (c) Hutin, M.; Schalley, C. A.; Bernardinelli, G.; Nitschke, J. R. *Chem.−Eur. J.* **2006**, *12*, 4069. (d) Wall, M.; Linkletter, B.; Williams, D. M.; Lebuis, A.; Hynes, R. C.; Chin, J. *J. Am. Chem. Soc.* **1999**, *121*, 4710.

(10) (a) Melton, D. L.; VanDerveer, D. G.; Hancock, R. D. *Inorg. Chem.* **2006**, *45*, 9306. (b) Cuevas, A.; Kremer, C.; Hummert, M.; Schumann, H.; Lloret, F.; Julve, M.; Faus, J. *Dalton Trans.* **2007**, 342. (c) Busby, M.; Gabrielsson, A.; Matousek, P.; Towrie, M.; Di Bilio, A. J.; Gray, H. B.; Vlček, A., Jr. *Inorg. Chem.* **2004**, *43*, 4994.

(11) (a) Mellace, M. G.; Fagalde, F.; Katz, N. E.; Crivelli, I. G.; Delgadillo, A.; Leiva, A. M.; Loeb, B.; Garland, M. T.; Baggio, R. *Inorg. Chem.* **2004**, *43*, 1100. (b) Harrop, T. C.; Olmstead, M. M.; Mascharak, P. K. *J. Am. Chem. Soc.* **2004**, *126*, 14714. (c) Harrop, T. C.; Olmstead, M. M.; Mascharak, P. K. *Inorg. Chem.* **2006**, *45*, 3424.

(12) (a) Lanznaster, M.; Heeg, M. J.; Yee, G. T.; McGarvey, B. R.; Verani, C. N. *Inorg. Chem.* **2007**, *46*, 72. (b) Armentano, D.; Munno, G. D.; Guerra, F.; Julve, M.; Lloret, F. *Inorg. Chem.* **2006**, *45*, 4626. (c) Yam, W. W. V.; Ko, C. C.; Zhu, N. Y. *J. Am. Chem. Soc.* **2004**, *126*, 12734.

(13) (a) Yuan, Y. F.; Cardinaels, T.; Lunstroot, K.; Van Hecke, K.; Meervelt, Van, L.; Gorller-Walrand, C.; Binnemans, K.; Nockemann, P. *Inorg. Chem.* **2007**, *46*, 5302. (b) Zeng, X. S.; Tavasli, M.; Perepichka, I. F.; Batsanov, A. S.; Bryce, M. R.; Chiang, C. J.; Rothe, C.; Monkman, A. P. *Chem.−Eur. J.* **2008**, *14*, 933. (c) Chen, X. Y.; Yang, X. P.; Holliday, B. J. *J. Am. Chem. Soc.* **2008**, *130*, 1546. (d) Shiotsuka, M.; Inui, Y.; Ito, M.; Onaka, S.; Ozeki, T.; Chiba, H. *Acta Crystallogr.* **2006**, *E62*, m980. (e) Shiotsuka, M.; Ogasawara, H.; Ito, M.; Onaka, S. *Acta Crystallogr., Sect. E* **2006**, *62*, m1410.

(14) Huang, W.; Masuda, G.; Maeda, S.; Tanaka, H.; Hino, T.; Ogawa, T. *Inorg. Chem.* **2008**, *47*, 468.

(15) Huang, W.; Tanaka, H.; Ogawa, T. *J. Phys. Chem. C* **2008**, *112*, 11513.

(16) Suzuki, H.; Kanbara, T.; Yamamoto, T. *Inorg. Chim. Acta* **2004**, *357*, 4335.

(17) (a) Goodbrand, H. B.; Hu, N. X. *J. Org. Chem.* **1999**, *64*, 670. (b) Lindley, J. *Tetrahedron* **1980**, *40*, 1433. (c) Fanta, P. E. *Synthesis.* **1974**, 1. (d) Hartwig, J. F. *Angew. Chem., Int. Ed.* **1998**, *37*, 2046.

(18) (a) Li, J. R.; Tao, Y.; Yu, Q.; Bu, X. H.; Sakamoto, H.; Kitagawa, S. *Chem.−Eur. J.* **2008**, *14*, 2771. (b) Du, M.; Bu, X. H.; Guo, Y. M.; Ribas, J.; Diaz, C. *Chem. Commun.* **2002**, 2550. (c) Bu, X. H.; Chen, W.; Du, M.; Biradha, K.; Wang, W. Z.; Zhang, R. H. *Inorg. Chem.* **2002**, *41*, 437. (d) Naumov, I. I.; Fu, H. *Phys. Rev. Lett.* **2005**, *95*, 247602. (e) Naumov, I. I.; Bellaiche, L.; Fu, H. *Nature (London)* **2004**, *432*, 737. (f) Gu, Z. G.; Zhou, X. H.; Jin, Y. B.; Zuo, J. L.; You, X. Z. *Inorg. Chem.* **2007**, *46*, 5462. (g) Wang, L.; You, W.; Huang, W. *J. Mol. Struct.* **2009**, *920*, 270.

(19) (a) Zhang, J.; Bu, X. H. *Angew. Chem., Int. Ed.* **2007**, *46*, 6115. (b) Chen, S. M.; Zhang, J.; Bu, X. H. *Inorg. Chem.* **2008**, *47*, 5567. (c) Zhang, J.; Yao, Y. G.; Bu, X. H. *Chem. Mater.* **2007**, *19*, 5083. (d) Zhang, J.; Chew, E.; Chen, S. M.; Pham, J. T. H.; Bu, X. H. *Inorg. Chem.* **2008**, *47*, 3495. (e) Zhang, J.; Liu, R.; Feng, P. Y.; Bu, X. H. *Angew. Chem., Int. Ed.* **2007**, *46*, 8388. (f) Zhang, J.; Bu, X. H. *Chem. Commun.* **2008**, 444. (g) Zhang, J; Chen, S. M.; Valle, H.; Wong, M.; Austria, C.; Cruz, M.; Bu, X. H. *J. Am. Chem. Soc.* **2007**, *129*, 14168.

(20) (a) Dybtsev, D. N.; Yutkin, M. P.; Peresypkina, E. V.; Virovets, A. V.; Serre, C.; Férey, G.; Fedin, V. P. *Inorg. Chem.* **2007**, *46*, 6843. (b) Rood, J. A.; Boggess, W. C.; Noll, B. C.; Henderson, K. W. *J. Am. Chem. Soc.* **2007**, *129*, 13675. (c) Zeng, M. H.; Wang, B.; Wang, X. Y.; Zhang, W. X.; Chen, X. M.; Gao, S. *Inorg. Chem.* **2006**, *45*, 7069. (d) Thuéry, P. *Eur. J. Inorg. Chem.* **2006**, 3646. (e) Kasuga, N. C.; Sugie, A.; Nomiya, K. *Dalton Trans.* **2007**, 3732. (f) Zhang, J.; Wu, T.; Feng, P. Y.; Bu, X. H. *Chem. Mater.* **2008**, *20*, 5457. (g) Zhang, J.; Chen, S. M.; Bu, X. H. *Angew. Chem., Int. Ed.* **2008**, *47*, 5434.

Scheme 2. Schematic Illustration of Different Conformations of 3,8-Diimidazol-1,10-phen Ligand in Different Coordination Modes with Cd(II) and Zn(II) Metal Ions

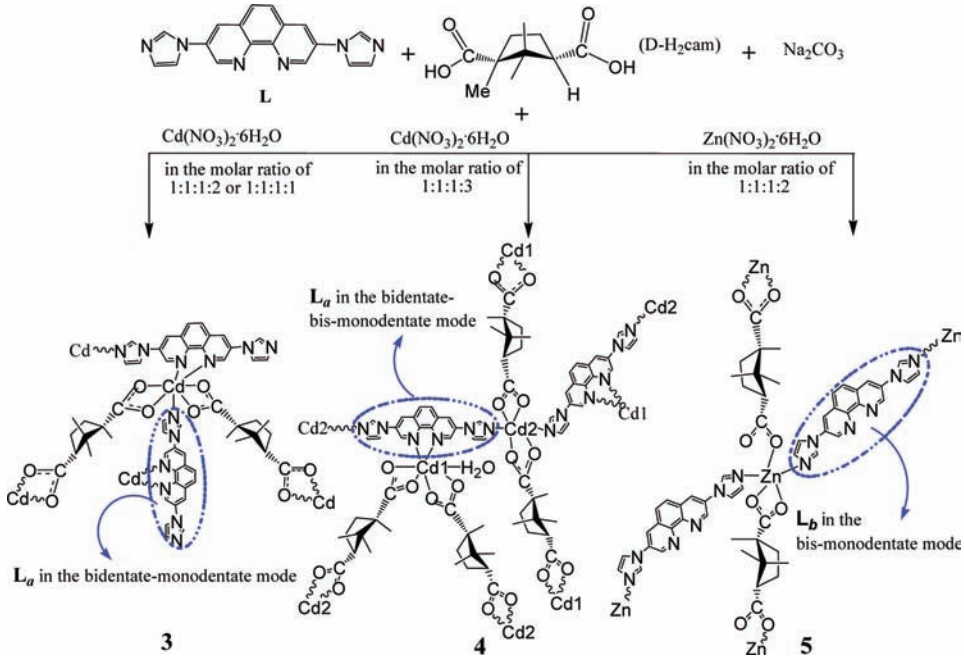

diimidazol-1,10-phen ligand (L_b) (**1**) and its dihydrate ($L_c \cdot 2H_2O$) (**2**). Furthermore, density functional theory (DFT) computations on comparing the different molecular conformations of this ligand and spectral, nonlinear optical, and thermal properties of related complexes are included.

Experimental Section

Materials and Measurements. All reagents were of analytical grade from commercial sources and were used without any further purification. Elemental analyses were measured with a Perkin-Elmer 1400C analyzer. Infrared spectra (FT-IR, 4000−400 cm^{-1}) were collected on a Nicolet FT-IR 170X spectrophotometer at 25 °C using KBr plates. ^1H NMR spectra were obtained in a Bruker 500 MHz NMR spectrometer. Electrospray ionization mass spectra (ESI-MS) were recorded on a Finnigan MAT SSQ 710 mass spectrometer in a scan range 100−1200 amu. Ultraviolet−visible (UV−vis) spectra were recorded on a Shimadzu UV-3100 double-beam spectrophotometer using a Pyrex cell with a path length of 10 mm at room temperature. Luminescence spectra were recorded on a Hitachi 850 fluorescent spectrophotometer at room temperature (25 °C). A pulsed Qswitched Nd:YAG laser with a wavelength of 1064 nm was used to generate the SHG signal. The backward-scattered SHG light was collected using a spherical concave mirror and passed through a filter that transmits only 532 nm radiation. Powder X-ray diffraction (XRD) measurements were performed on a Philips X′pert MPD Pro X-ray diffractometer using Cu $K\alpha$ radiation (λ = 0.15418 nm), in which the X-ray tube was operated at 40 kV and 40 mA at room temperature. Thermogravimetric analysis (TGA) data were recorded by a CA Instruments DTA-TGA 2960 type simultaneous analyzer heating from 20 °C to 800 °C at 10 °C/min. The autoclave equipped with a 25 mL Teflon cup used for preparing complex was produced by Binghai Xian Zhenghong Plastic Factory in Jiangsu province.

Ligand Synthesis. 3,8-Diimidazol-1,10-phen. 3,8-Dibromo-1,10-phen[21] (1.014 g, 3.0 mmol), imidazole (0.681 g, 10.0 mmol), K_2CO_3 (0.691 g, 5.0 mmol), and anhydrous $CuSO_4$ (0.012 g, 0.075 mmol) were mixed and heated at 180 °C under N_2 for 4 h. After being cooled to room temperature, the resultant mixture was washed with water and the residue was extracted with $CHCl_3$ (5 × 30 mL). The organic layer was separated, dried over anhydrous sodium sulfate, evaporated to dryness, and recrystallized from water and ethanol. Yield: 70%. Mp >220 °C. Elemental anal. Calcd for $C_{18}H_{12}N_6$: C, 69.22; H, 3.87; N, 26.91. Found: C, 69.18; H, 3.98; N, 26.88%. Main FT-IR absorptions (KBr pellets, ν, cm^{-1}): 3116 (m), 1615 (m), 1497 (s), 1439 (m), 1406 (w), 1373 (w), 1321 (m), 1298 (s), 1259 (m), 1105 (m), 1067 (m), 1032 (w), 1004 (m), 903 (m), 883 (m), 799 (w), 726 (m), and 652 (m). ^1H NMR (500 MHz, CD_3OD, 298K, TMS, ppm): δ 9.1 (2H, phen), 8.76 (2H, phen), 8.52 (2H, phen), 8.15 (2H, imidazole), 7.93 (2H, imidazole), and 7.32 (2H, imidazole). ESI-MS, *m/z* (%): 313 (100), $[HL]^+$; 335 (50), $[NaL]^+$. UV−vis (CH_3OH) λ_{max} = 317 and 262 nm. The light yellow needlelike single crystals of L_b (**1**) suitable for X-ray diffraction determination were grown from a solution of methanol by slow evaporation in air at room temperature, while the colorless needle-like single crystals of $L_c \cdot 2H_2O$ (**2**) suitable for X-ray diffraction determination were grown from a mixed solution of methanol and water (2:1) by slow evaporation in air at room temperature. Main FT-IR absorptions (KBr pellets, ν, cm^{-1}) for **2**: 3441 (b), 3153 (m), 3117 (m), 3057(m), 2999 (w), 1614 (s), 1505 (s), 1483 (m), 1443 (m), 1407 (w), 1372 (w), 1322 (s), 1302(s), 1246 (s), 1108 (m), 1069 (m), 1034 (m), 1007 (m), 916 (m), 820 (m), 791 (m), 741 (m), and 729 (m).

Preparation of the Complexes. $[Cd_2(D\text{-}cam)_2L_{a2}]\cdot(H_2O)_6$ (3). A mixture of D-H_2cam (0.010 g, 0.05 mmol), Na_2CO_3 (0.005 g, 0.05 mmol), 3,8-diimidazol-1,10-phen (0.016 g, 0.05 mmol), and $Cd(NO_3)_2 \cdot 6H_2O$ (0.035 g, 0.10 mmol) in a molar ratio of 1:1:1:2 and H_2O (8 mL) was sealed in a 25 mL Teflon cup, heated at 140 °C for 3 days, and then cooled to room temperature giving light

(21) Saitoh, Y.; Koizumi, T.; Osakada, K.; Yamamoto, T. *Can. J. Chem.* **1997**, *75*, 1337.

Table 1. Crystal Data and Structure Refinements for **1**−**5**

	1	2	3	4	5
empirical formula	$C_{18}H_{12}N_6$	$C_{18}H_{16}N_6O_2$	$C_{56}H_{64}Cd_2N_{12}O_{14}$	$C_{38}H_{42}Cd_2N_6O_9$	$C_{56}H_{62}Zn_2N_{12}O_{13}$
fw	312.34	348.37	1354.02	951.58	1241.92
cryst syst	monoclinic	triclinic	orthorhombic	monoclinic	monoclinic
space group	$P2_1/c$	$P\bar{1}$	$P2_12_12_1$	$P2_1$	$P2_1$
a (Å)	11.107(1)	7.194(1)	16.902(3)	6.4751(8)	10.592(4)
b (Å)	9.464(1)	8.428(1)	18.351(2)	23.110(3)	22.306(8)
c (Å)	13.306(1)	14.081(2)	18.787(3)	12.560(2)	13.120(5)
α (deg)	90	87.277(2)	90	90	90
β (deg)	91.210(3)	81.357(1)	90	100.715(2)	100.813(4)
γ (deg)	90	73.104(2)	90	90	90
V (Å^3)	1398.4(3)	807.53(19)	5827.1(17)	1846.6(4)	3045(2)
Z, D_{calcd} (Mg/m^3)	4, 1.484	2, 1.433	4, 1.543	2, 1.711	2, 1.355
F(000)	648	364	2768	960	1292
μ (mm^{-1})	0.095	0.099	0.805	1.217	0.858
h_{min}/h_{max}	−10/13	−8/8	−19/20	−7/7	−12/12
k_{min}/k_{max}	−11/11	−10/9	−21/21	−27/26	−11/26
l_{min}/l_{max}	−15/15	−13/16	−22/12	−14/14	−15/15
params	217	235	763	483	727
final R indices [$I > 2\sigma(I)$]	$R_1 = 0.0696$, $wR_2 = 0.1434$	$R_1 = 0.0451$, $wR_2 = 0.0898$	$R_1 = 0.0489$, $wR_2 = 0.0721$	$R_1 = 0.0558$, $wR_2 = 0.1393$	$R_1 = 0.0715$, $wR_2 = 0.1630$
R indices (all data)	$R_1 = 0.0749$, $wR_2 = 0.1463$	$R_1 = 0.1047$, $wR_2 = 0.1067$	$R_1 = 0.0611$, $wR_2 = 0.0751$	$R_1 = 0.0679$, $wR_2 = 0.1474$	$R_1 = 0.1330$, $wR_2 = 0.1808$
GOF on F^2	1.06	0.78	1.07	1.08	0.98
Δ (e Å^{-3}) (max, min)	0.27/−0.23	0.19/−0.23	0.67/−0.46	1.21/−1.25	0.48/−0.36
flack parameter			−0.03(2)	−0.07(5)	0.03(2)

yellow microcrystals. Yield: 0.052 g (76%) based on metal. Anal. Calcd for $C_{56}H_{64}Cd_2N_{12}O_{14}$: C, 69.22; H, 12.10; N, 26.91%. Found: C, 69.32; H, 12.04; N, 26.80%. Main FT-IR absorptions (KBr pellets, ν, cm^{-1}): 3441 (w), 3096 (w), 2965 (w), 1613 (m), 1551 (s), 1502 (S), 1480 (w), 1441 (m), 1393 (m), 1307 (m), 1256 (w), 1107 (w), 1072 (m), 1034 (w), 1005 (m), 932 (w), 886 (w), 786 (w), 727 (m), and 654 (m). ESI-MS, m/z (%): 697 (100), [CdL$_a$(D-Hcam)(CH$_3$CN)(CH$_3$OH)]$^+$; 954 (20), [CdL$_{a2}$(D-Hcam)(H$_2$O)]$^+$. UV−vis (DMF) λ_{max} = 321 and 275 nm.

[Cd$_2$(D-cam)$_2$(L$_a$)(H$_2$O)] (4). A mixture of D-H$_2$cam (0.010 g, 0.05 mmol), Na$_2$CO$_3$ (0.005 g, 0.05 mmol), 3,8-diimidazol-1,10-phen (0.016 g, 0.05 mmol), and Cd(NO$_3$)$_2$·6H$_2$O (0.052 g, 0.15 mmol) in a molar ratio of 1:1:1:3 and H$_2$O (10 mL) was sealed in a 25 mL Teflon cup, heated at 140 °C for 3 days, then cooled to room temperature, giving light yellow microcrystals. Yield: 0.050 g (70%) based on metal. Anal. Calcd for $C_{38}H_{42}Cd_2N_6O_9$: C, 47.96; H, 4.45; N, 8.83%. Found: C, 48.05; H, 4.40; N, 8.72%. Main FT-IR absorptions (KBr pellets, ν, cm^{-1}): 3379 (w), 3114 (w), 3066 (w), 2963 (m), 1616 (m), 1544 (s), 1513 (s), 1451 (w), 1403 (m), 1366 (w), 1299 (w), 1272 (w), 1176 (w), 1122 (m), 1070 (m), 1003 (w), 920 (m), 811 (m), 751 (w), 720 (w), and 641 (m). ESI-MS, m/z (%): 570 (100), [CdL$_{a2}$(D-Hcam)$_2$(CH$_3$OH)]$^{2-}$/2; 273 (69), [Cd(D-cam)$_2$(H$_2$O)$_2$]$^{2-}$/2. UV−vis (DMF) λ_{max} = 323 and 277 nm.

[Zn$_2$(D-cam)$_2$(L$_b$)$_2$]·(H$_2$O)$_5$ (5). A mixture of D-H$_2$cam (0.010 g, 0.05 mmol), Na$_2$CO$_3$ (0.005 g, 0.05 mmol), 3,8-diimidazol-1,10-phen (0.016 g, 0.05 mmol), and Zn(NO$_3$)$_2$·6H$_2$O (0.030 g, 0.10 mmol) in a molar ratio of 1:1:1:2 and H$_2$O (10 mL) was sealed in a 25 mL Teflon cup, heated at 140 °C for 3 days, and then cooled to room temperature, giving light yellow microcrystals. Yield: 0.047 g (75%) based on metal. Anal. Calcd for $C_{56}H_{62}Zn_2N_{12}O_{13}$: C, 54.16; H, 5.03; N, 13.53%. Found: C, 54.23; H, 4.99; N, 13.58%. Main FT-IR absorptions (KBr pellets, ν, cm^{-1}): 3413 (s), 3142 (m), 2966 (m), 1588 (s), 1511 (s), 1447 (m), 1366 (s), 1314 (w), 1254 (w), 1125 (m), 1072 (m), 1036 (w), 1003 (w), 942 (w), 906 (w), 797 (w), 729 (m), and 650 (m). ESI-MS, m/z (%): 414 (100), [ZnL$_b$(D-H$_2$cam)(CH$_3$OH)(H$_2$O)]$^{2+}$/2; 673 (50), [ZnL$_b$(D-Hcam)(CH$_3$OH)(C$_2$H$_5$OH)(H$_2$O)]$^+$. UV−vis (DMF) λ_{max} = 321 and 277 nm.

Crystallography. All single-crystal samples were covered with glue and mounted on glass fibers for data collection with Mo $K\alpha$ radiation (λ = 0.71073 Å) on a Bruker SMART 1000 diffractometer equipped with a CCD camera. Data collection was performed by using SMART program and cell refinement and data reduction were made with the SAINT program.[22] All the structures were solved by directed method and refined on F^2 by using full-matrix least-squares methods with SHELXTL version 6.10.[23] All non-H atoms were anisotropically refined. All hydrogen atoms were inserted in the calculated positions, assigned fixed isotropic thermal parameters at 1.2 times the equivalent isotropic U of the atoms to which they are attached (1.5 times for the methyl groups and oxygen atoms), and allowed to ride on their respective parent atoms. All calculations were carried out on a PC computer with the SHELXTL PC program package and molecular graphics were drawn by using XSHELL and DIAMOND softwares. The U_{eq} parameters of some camphorate units in complexes **3**−**5** are relatively large, mainly because of the low quality of the single-crystal samples; however, their structural models are believed to be reliable from the viewpoint of chemistry. Details of the data collection and refinement for **1**−**5** are given in Table 1, whereas the selective bond lengths and angles of these complexes are listed in Table 2.

Results and Discussion

Synthesis and Electronic Spectral Characterizations. 3,8-Diimidazol-1,10-phen was synthesized by the carbon−nitrogen bond cross-coupling reaction between 3,8-dibromo-1,10-phen and imidazole in a high yield using Ullmann condensation methods.[17] Single-crystal samples of **1** and **2** with or without lattice water molecules were grown from different solvents. It is found that metal complexes **3**, **4**, and **5** can be yielded by using different molar ratios of four starting materials in the process of metal-ion complexation (Scheme 2) and the experimental results are easy to be reproduced. In addition, it is suggested that the difference in the radii of Cd(II) and Zn(II) ions contributes to forming different networks of **3**−**5**

(22) *SMART and SAINT, Area Detector Control and Integration Software*; Siemens Analytical X-ray Systems Inc.: Madison, WI, 2000.
(23) Sheldrick, G. M. *SHELXTL*, version 6.10, Siemens Industrial Automation: Madison, WI, 2000.

Table 2. Selected Bond Distances (Å) and Bond angles (deg) in **1**−**5**[a]

		1	
C2−N3	1.422(3)	C13−N3	1.350(3)
C9−N5	1.424(3)	C16−N5	1.354(3)
N4−C13−N3	112.6(2)	N6−C16−N5	112.2(2)
		2	
C2−N3	1.424(3)	C13−N3	1.346(3)
C9−N5	1.422(3)	C16−N5	1.362(3)
N4−C13−N3	113.5(2)	N6−C16−N5	112.5(3)
		3	
Cd1−N4^{A}	2.289(5)	Cd2−N12^{C}	2.313(5)
Cd1−O7^{B}	2.312(4)	Cd2−O4	2.313(4)
Cd1−O1	2.363(4)	Cd2−O6	2.390(4)
Cd1−N1	2.400(4)	Cd2−O3	2.424(4)
Cd1−O8^{B}	2.423(4)	Cd2−N8	2.430(4)
Cd1−O2	2.459(4)	Cd2−N7	2.448(5)
Cd1−N2	2.557(5)	Cd2−O5	2.462(4)
N4^{A}−Cd1−O7^{B}	146.0(2)	N12^{C}−Cd2−O4	149.4(2)
N4^{A}−Cd1−O1	102.7(2)	N12^{C}−Cd2−O6	104.6(2)
O7^{B}−Cd1−O1	106.0(2)	O4−Cd2−O6	96.8(2)
N4^{A}−Cd1−N1	103.4(2)	N12^{C}−Cd2−O3	94.8(2)
O7^{B}−Cd1−O8^{B}	54.9(1)	O4−Cd2−O3	54.7(2)
N1−Cd1−O8^{B}	141.9(1)	O4−Cd2−N8	100.8(2)
O1−Cd1−O2	52.7(1)	O3−Cd2−N8	137.6(1)
N1−Cd1−O2	132.5(2)	O6−Cd2−N7	148.1(2)
O1−Cd1−N2	146.5(2)	O3−Cd2−N7	77.9(2)
N1−Cd1−N2	66.7(1)	O6−Cd2−O5	53.1(1)
O2−Cd1−N2	157.9(2)	N7−Cd2−O5	157.8(1)
		4	
Cd1−O1	2.653(11)	Cd2−O9	2.285(8)
Cd1−O2	2.211(11)	Cd2−N6	2.303(8)
Cd1−O3	2.357(9)	Cd2−N4^{E}	2.307(9)
Cd1−O6^{D}	2.192(9)	Cd2−O5^{F}	2.305(11)
Cd1−O7^{D}	2.816(9)	Cd2−O4^{F}	2.400(8)
Cd1−N1	2.379(8)	Cd2−O8	2.439(8)
Cd1−N2	2.436(8)		
O6^{D}−Cd1−O2	104.5(4)	N6−Cd2−N4^{E}	98.7(3)
O6^{D}−Cd1−O3	91.2(4)	O9−Cd2−O5^{F}	104.7(4)
O2−Cd1−O3	78.8(4)	N6−Cd2−O5^{F}	107.1(4)
O6^{D}−Cd1−N1	129.4(3)	N4^{E}−Cd2−O5^{F}	94.5(4)
O2−Cd1−N1	107.3(4)	O9−Cd2−O4^{F}	108.2(4)
O3−Cd1−N1	132.7(3)	N4^{E}−Cd2−O4^{F}	147.7(3)
O6^{D}−Cd1−N2	97.0(3)	O5^{F}−Cd2−O4^{F}	53.8(4)
O2−Cd1−N2	151.5(4)	O9−Cd2−O8	52.9(3)
N1−Cd1−N2	71.1(3)	N4^{E}−Cd2−O8	119.0(3)
O9−Cd2−N6	147.8(3)	O5^{F}−Cd2−O8	132.7(5)
		5	
Zn1−O1	1.934(8)	Zn2−O5	1.915(7)
Zn1−O2	2.855(9)	Zn2−O6	2.782(7)
Zn1−O8^{G}	1.943(9)	Zn2−N6	2.001(13)
Zn1−N10	2.033(13)	Zn2−N12^{H}	1.996(10)
Zn1−N4	2.028(14)	Zn2−O3^{I}	1.966(12)
O1−Zn1−O8^{G}	108.5(4)	O5−Zn2−N6	124.1(5)
O1−Zn1−N10	114.2(4)	O5−Zn2−N12^{H}	108.6(4)
O8^{G}−Zn1−N10	117.6(5)	N6−Zn2−N12^{H}	103.5(4)
O1−Zn1−N4	116.4(5)	O5−Zn2−O3^{I}	111.2(4)
N10−Zn1−N4	104.0(5)	N12^{H}−Zn2−O3^{I}	118.6(6)

[a] Symmetric codes. A: $0.5 + x$, $0.5 - y$, $1 - z$. B: x, $1 + y$, z. C: $-0.5 + x$, $-0.5 - y$, $1 - z$. D: $-2 + x$, y, $-1 + z$. E: $1 - x$, $0.5 + y$, $2 - z$. F: $2 - x$, $0.5 + y$, $1 - z$. G: $2 - x$, $0.5 + y$, $-z$. H: x, $-1 + y$, $-1 + z$. I: $1 - x$, $-0.5 + y$, $1 - z$.

where 3,8-diimidazol-1,10-phen ligand shows different molecular conformations, coordination numbers, and architectures.

The UV−vis spectrum of free 3,8-diimidazol-1,10-phen molecule in methanol exhibits two absorption bands at 262 and 317 nm, respectively. The first one is assigned to an intraring $\pi-\pi^*$ transition in 3,8-diimidazol-1,10-phen, and the second to an inter-ring $\pi-\pi^*$ transition within the conjugated π system. Because of the low solubility of complexes **3**−**5** in methanol, DMF was used as the solvent to record the UV−vis spectra. The absorption peaks at high-energy band (275 and 321 nm in **3**, 277 and 323 nm in **4**, 277 and 321 nm in **5**) have been red-shifted to a different extent compared with the free ligand, indicative of the influence of metal-ion complexation. Three complexes have no absorption in the low-energy band because of the same d^{10} electronic configuration of Zn(II) and Cd(II) ions.[24]

DFT Computational Studies for Different Isomers of 3,8-Diimidazol-1,10-phen in the trans/trans, cis/cis, and trans/cis Conformations. All the DFT calculations were carried out with the Gaussian 03, revision C.02, programs[25] using the MPW1PW91 method and the LanL2DZ basis set. The fixed atom coordinates of **1** and **2**, originating from the structural parameters determined by the X-ray diffraction method, were used as the input file for the total energy calculation.

DFT calculations have been carried out to compare the energy differences between the single-crystal and the energy-minimized structures for 3,8-diimidazol-1,10-phen with the imidazol rings in the trans/trans, trans/cis, and cis/cis conformations relative to the central phen plane (Scheme 1). The total energy for the single-crystal structure of **1**, where the two nitrogen atoms of imidazol rings are in the cis/trans conformation relative to the two nitrogen atoms of phen unit, is −2677497.61 KJ/mol, whereas the energy-minimized structure has the total energy of −2678608.40 KJ/mol. In contrast, the total energy for the single-crystal structure of **2** in the cis/cis conformation is −2677917.10 KJ/mol and that for the energy-minimized structure is −2678607.56 KJ/mol. The total energy for the energy-minimized structure of trans/trans isomer is −2678608.64 KJ/mol. Large energy gaps between the single-crystal structure and the energy-minimized structure for **1** (1110.79 KJ/mol) and **2** (690.46 KJ/mol) reflects the contribution of supramolecular interactions between molecules in the solid state such as hydrogen bonding and $\pi-\pi$ stacking.

The sequence for the thermal stability of energy-minimized structures of 3,8-diimidazol-1,10-phen in these configurations is trans/trans > trans/cis > cis/cis isomers. However, the energy gaps of three isomers (0.84 KJ/mol between the cis/cis and trans/cis isomers and 0.20 KJ/mol between the trans/cis and trans/trans isomers) are not so large, which means that all of them are accessible isomers and they are

(24) Lever, A. B. P. *Inorganic Electronic Spectroscopy*, 2nd ed.; Elsevier: Amsterdam, 1984.

(25) Frisch, M. J.; Trucks, G. W.; Schlegel, H. B.; Scuseria, G. E.; Robb, M. A.; Cheeseman, J. R.; Montgomery, J. A.; Vreven, Jr T.; Kudin, K. N.; Burant, J. C.; Millam, J. M.; Iyengar, S. S.; Tomasi, J.; Barone, V.; Mennucci, B.; Cossi, M.; Scalmani, G.; Rega, N.; Petersson, G. A.; Nakatsuji, H.; Hada, M.; Ehara, M.; Toyota, K.; Fukuda, R.; Hasegawa, J.; Ishida, M.; Nakajima, T.; Honda, Y.; Kitao, O.; Nakai, H.; Klene, M.; Li, X.; Knox, J. E.; Hratchian, H. P.; Cross, J. B.; Adamo, C.; Jaramillo, J.; Gomperts, R.; Stratmann, R. E.; Yazyev, O.; Austin, A. J.; Cammi, R.; Pomelli, C.; Ochterski, J. W.; Ayala, P. Y.; Morokuma, K.; Voth, G. A.; Salvador, P.; Dannenberg, J. J.; Zakrzewski, V. G.; Dapprich, S.; Daniels, A. D.; Strain, M. C.; Farkas, O.; Malick, D. K.; Rabuck, D.; Raghavachari, K.; Foresman, J. B.; Ortiz, J. V.; Cui, Q.; Baboul, A. G.; Clifford, S.; Cioslowski, J.; Stefanov, B. B.; Liu, G.; Liashenko, A.; Piskorz, P.; Komaromi, I. ; Martin, R. L.; Fox, D. J.; Keith, T.; Al-Laham, M. A.; Peng, C. Y.; Nanayakkara, A.; Challacombe, M.; Gill, P. M. W.; Johnson, B.; Chen, W.; Wong, M. W.; Gonzalez, C.; Pople, J. A. *Gaussian 03, Revision C.02*; Gaussian, Inc.; Pittsburgh, PA, 2004.

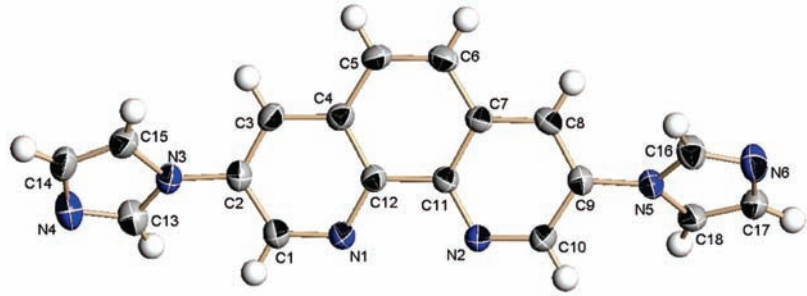

Figure 1. Thermal Ellipsoid Plot (ORTEP) diagram (30% thermal probability level ellipsoids) of the molecular structure of **1** with the atom-numbering scheme.

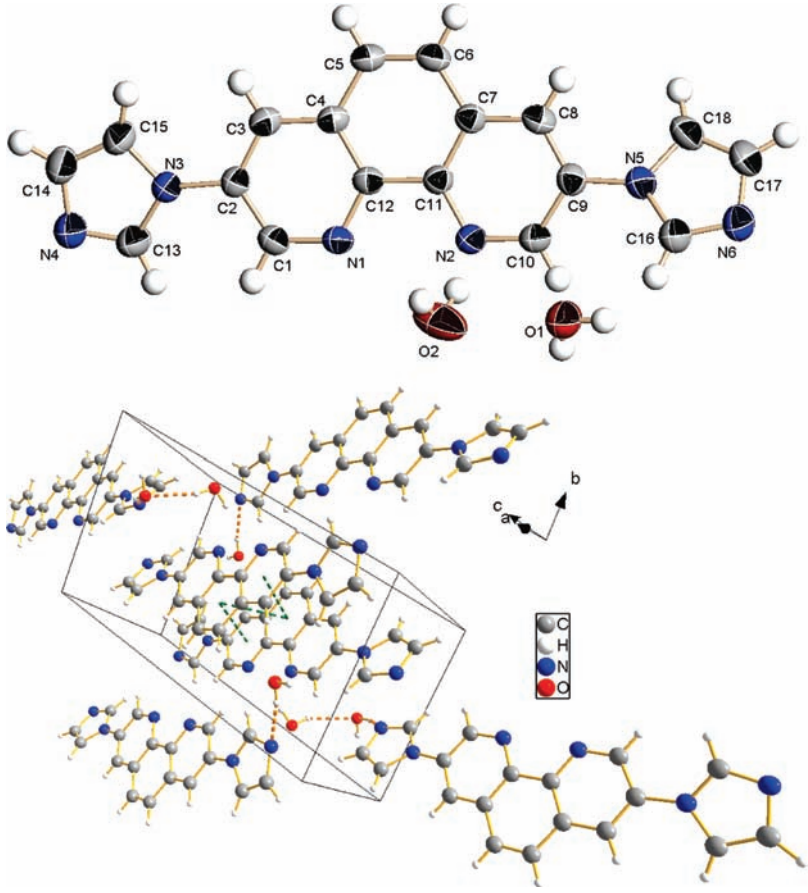

Figure 2. (a) ORTEP diagram (30% thermal probability level ellipsoids) of the molecular structure of **2** with the atom-numbering scheme. (b) View of the hydrogen bonding and $\pi-\pi$ stacking interactions in **2**.

interconvertible under certain circumstances. For instance, all three possible isomers have been observed in the molecular structures of **1**−**5** in this work.

For all three energy-minimized structures, two side imidazol rings are parallel with the central phen ring to maximize the conjugated π system, which is different from our previously calculated 3,8-di(thiophen-2′,2″-yl)-1,10-phen isomers where both thiophene rings are staggered at each side of the phen plane with the dihedral angles of 14.5(2), 17.8(2), and 21.5(2)°.[26] Nevertheless, these dihedral angles can be changed via the rotation of the C−N single bonds to some extend after the metal-ion complexation and they can be reflected in their UV−vis spectra.

(26) Huang, W.; Wang, L.; Tanaka, H.; Ogawa, T. *Eur. J. Inorg. Chem* **2009**, 1321.

Crystal Structures of L_b (1) and $L_c \cdot 2H_2O$ (2). The molecular structures of **1** and **2** with the atom-numbering scheme are shown in Figure 1 and Figure 2a, respectively. X-ray diffraction studies with compound **1** indicate that it crystallizes in the monoclinic space group $P2_1/c$ and the two side imidazole rings are not coplanar to the central phen ring. Instead, they are staggered at each side of the phen plane with the dihedral angles of 37.1(2) and 43.3(2)°, respectively. The two nitrogen atoms of imidazole rings point to the opposite direction (in the cis/trans configuration) to the two nitrogen atoms of phen unit. There are weak C−H···N hydrogen bonds (Table 3) but no $\pi-\pi$ stacking interactions in the crystal packing of **1**.

X-ray diffraction studies on **2** indicate that it crystallizes in the triclinic space group $P\bar{1}$ and two water molecules are

Table 3. Intermolecular Hydrogen-Bonding Parameters (Å, deg) in **1**−**5**[a]

D−H···A	D−H	H···A	D···A	∠DHA
	1			
C15−H15···N1^{A}	0.93	2.58	3.51(1)	177
C18−H18···N2^{B}	0.93	2.49	3.40(1)	166
	2			
O1−H1A···N6^{C}	0.85	2.03	2.79(1)	148
O1−H1B...N4^{B}	0.85	2.08	2.92(1)	168
O2−H2B···O1^{D}	0.85	2.15	2.87(1)	142
C1−H1...N1^{B}	0.93	2.61	3.36(1)	137
C3−H3···O1^{E}	0.93	2.48	3.38(1)	165
C8−H8···O2^{F}	0.93	2.31	3.20(1)	160
	3			
O10−H10A···O1^{G}	0.85	2.52	3.20(1)	138
O11−H11B···O14^{F}	0.85	2.42	2.95(1)	122
O11−H11B···N9^{H}	0.85	2.54	3.20(1)	136
O14−H14A···O11^{I}	0.85	2.36	2.95(1)	128
O14−H14B···O13^{J}	0.85	2.48	3.19(1)	141
	4			
O3−H3B···O7^{K}	0.85	2.10	2.81(2)	141
	5			
O10−H10B···N7^{L}	0.85	2.52	3.21(2)	139
O10−H10B···N8^{L}	0.85	2.30	2.99(2)	139
O12−H12A···O4^{M}	0.85	1.77	2.56(5)	154
O14−H14B···O7^{N}	0.85	1.98	2.72(8)	145

[a] Symmetric codes. A: $-x$, $0.5 + y$, $0.5 - z$. B: $1 - x$, $-y$, $1 - z$. C: $2 - x$, $1 - y$, $-z$. D: $-1 + x$, y, z. E: $1 - x$, $1 - y$, $1 - z$. F: x, $1 + y$, z. G: $1 - x$, $0.5 + y$, $0.5 - z$. H: $1.5 - x$, $1 - y$, $-0.5 + z$. I: x, $-1 + y$, z. J: $0.5 + x$, $0.5 - y$, $1 - z$. K: $-1 + x$, y, $-1 + z$. L: $1 - x$, $-0.5 + y$, $1 - z$. M: $1 + x$, y, z. N: $-1 + x$, y, $1 - z$.

included in each asymmetric unit. The two side imidazole rings are also not coplanar to the central phen ring with the smaller dihedral angles of 22.7(2) and 12.9(2)°, respectively. However, the molecular conformation of **2** is different from that of **1** where the two nitrogen atoms of imidazole rings point to the same direction (in the cis/cis configuration) to the two nitrogen atoms of phen unit. The difference in their configurations may originate from the stronger hydrogen bonding interactions in **2** because there are not only weak C−H···N and C−H···O hydrogen bonds but also strong O−H···N and O−H···O hydrogen bonds in the crystal packing of **2** (Figure 2b). It is noted that all the phen moieties in **1** and **2** are parallel and packed in an offset way, but adjacent molecules are shifted to different extend and only $\pi-\pi$ stacking interactions in the case of **2** are found between contiguous phen units with the centroid-centroid separations in the range of 3.599(3)−3.859(3) Å (Figure 2b).

Crystal Structure of $[Cd_2(D\text{-cam})_2(L_a)_2]\cdot(H_2O)_6$ (3). The asymmetric unit of **3** contains two Cd(II) cations, two 3,8-diimidazol-1,10-phen ligands in the trans/trans conformation (L_a), two D-cam dianionic ligands, and six lattice water molecules. As shown in Figure 3, each Cd(II) ion is seven-coordinated by two chelating nitrogen atoms from one L_a ligand, one nitrogen atom from the imidazole ring of the other with a dihedral angle of 39.3(2)° between the phen rings of two L_a ligands, and four oxygen atoms from two D-cam ligands forming a slightly distorted pentagonal bipyramid. Each L_a acts as a bidentate-monodentate ligand and the two side imidazole rings are not coplanar to the central phen ring with the dihedral angles of 40.3(2) and 50.7(2)°, where the two nitrogen atoms of imidazole rings point to the same direction (trans/trans) opposite to the two nitrogen atoms of phen unit. A 1D helical chain comes into being where two Cd(II) ions and one and a half 3,8-diimidazol-1,10-phen ligands are connected in a continuous T-shaped fashion (phen/Cd(II)/imi) constituting every helical cycle with the pitch length of 16.909(5) Å (Figure 4a). In addition, each D-cam acts as a bis- bidentate ligand coordinating to two Cd(II) centers and linking neighboring phen/Cd(II)/imi helical chains into a 2D lamellar coordination polymer along the *ab* plane (Figure 4b). $\pi-\pi$ Stacking interactions between adjacent side pyridyl rings of L_a ligands within the 2D layers are found with the centroid−centroid separations of 3.811(4) and 3.933(4) Å. Moreover, intralayer and interlayer O−H···O and O−H···N hydrogen bonds (Table 3) are present, cooperatively forming a 3D network in the case of **3**.

Crystal Structure of $[Cd_2(D\text{-cam})_2(L_a)(H_2O)]$ (4). The asymmetric unit of **4** consists of two Cd(II) cations, two D-cam dianionic ligands, one 3,8-diimidazol-1,10-phen ligand in the trans/trans conformation (L_a), and one coordination water molecule (Figure 5). The coordination geometry for Cd1 and Cd2 ions is slightly different. Namely, the Cd1 ion is seven-coordinated by two chelating nitrogen atoms from one L_a ligand, four oxygen atoms from two D-cam dianionic ligands, and one water molecule to form a distorted pentagonal bipyramid, whereas the Cd2 ion is six-coordinated by two imidazole nitrogen atoms from two L_a ligands with a dihedral angle of 88.5(3)° between the phen rings of these two L_a ligands and four oxygen atoms from two D-cam ligands to form a distorted octahedral configuration.

The conformation of the L_a ligand in complex **4** is the same as that in complex **3**. However, L_a acts as a bidentate-bis-monodentate ligand here instead of a bidentate-monodentate ligand in **3**, and the smaller dihedral angles (7.3(4) and 31.2(4)°) between the two side imidazole rings and the central phen ring are observed. In the entire structure of **4**, each L_a ligand coordinates to three Cd(II) cations; meanwhile, each carboxylic group of D-cam ligand connects with two Cd(II) cations in a bidentate bridging fashion.

The most fascinating structural feature of **4** is that two kinds of single-strand helical chains are present sharing the same metal atoms along the helical *b* axis (Figure 7). Besides the covalent helix originating from the D-cam ligands where four Cd(II) ions and four bridging D-cam dianionic moieties constitute every helical cycle (Figure 6a), there is the second type of helix originating from the 3,8-diimidazol-1,10-phen ligands where four Cd(II) ions and two 3,8-diimidazol-1,10-phen ligands constitute every helical cycle (Figure 6b). Different from **3**, a new type of imi/Cd^{II}/imi helix is produced where the 3,8-diimidazol-1,10-phen ligands are coordinated with the Cd(II) ions by both imidazol N atoms in every helical unit. The common helical pitch of these two kinds of helices is 23.110(8) Å, which is much longer than those of helices formed by D-cam ligands including **3** and metal sites by Bu and co-workers where no additional helix-generating molecules are present.[19a] The above-mentioned two types single-strand helices are extended by bridging D-cam and 3,8-diimidazol-1,10-phen ligands, respectively, down the *a* and *c* axes constituting a 3D homohelical network

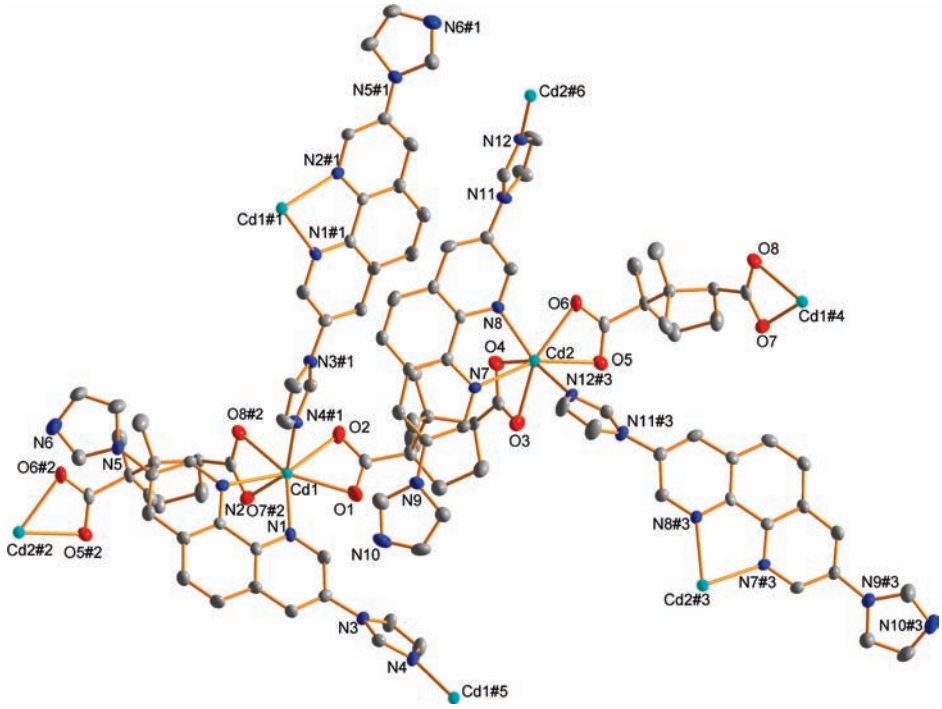

Figure 3. ORTEP drawing of **3** showing 30% probability level ellipsoids (hydrogen atoms and water molecules are omitted for clarity). Symmetry codes: #1: 0.5 + *x*, 0.5 − *y*, 1 − *z*; #2: *x*, 1 + *y*, *z*; #3: −0.5 + *x*, −0.5 − *y*, 1 − *z*; #4: *x*, −1 + *y*, *z*; #5: −0.5 + *x*, 0.5 − *y*, 1 − *z*; #6: 0.5 + *x*, −0.5 − *y*, 1 − *z*.

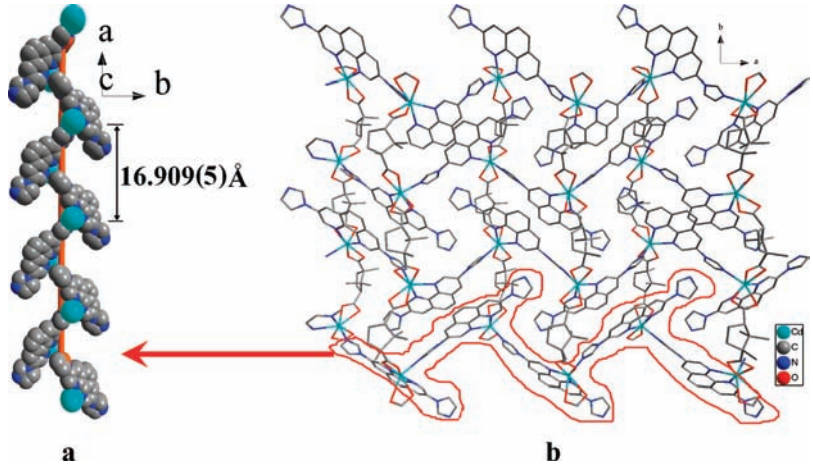

Figure 4. Perspective view of (a) the phen/Cd(II)/imi helical chain and (b) homochiral 2D layer in **3**.

(Figure 8). Compared with the 2D structure of **3**, one can see that the increase in the molar ratios of metals and ligands induces the progressive increase in dimensions of the ultimate structures.

Crystal Structure of $[Zn_2(D\text{-cam})_2(L_b)_2]\cdot(H_2O)_5$ (5). The asymmetric unit of **5** includes two Zn(II) cations, two D-cam dianionic, two 3,8-diimidazol-1,10-phen ligands in the cis/trans conformation (L_b) and five water molecules free of coordinative bond. Each Zn(II) ion is five-coordinated by two nitrogen atoms from two imidazole rings of two L_b ligands, two oxygen atoms from a bidentate D-cam ligand, and one oxygen atom from another D-cam ligand (Figure 8). Similarly, each D-cam ligand bridges two adjacent Zn(II) ions to form a single-strand helical chain but with a shorter helical pitch of 18.343(9) Å, where two Zn(II) ions and two D-cam ligands constitute every helical cycle (Figure 9a). Nevertheless, different from **3** and **4**, the 3,8-diimidazol-1,10-phen ligand in **5** serves as a bis-monodentate linear bridging ligand, but the dihedral angles between the two side imidazole rings and the central phen ring (7.8(4) and 34.4(4)°) are analogous to **4**. The D-cam involved single-strand helices are connected by the μ_2−bridging L_b ligands constructing a 3D framework, where the L_b ligands are packed in a zigzag way with the dihedral angle of 77.3(4)° (Figure 9b). Moreover, $\pi-\pi$ stacking interactions are found between pyridyl rings of the L_b ligands from neighboring zigzag layers with a centroid-centroid separation of 3.634(8) Å.

Thermal Analysis. The thermogravimetric analyses (TGA) of the free ligand (**1**) and coordination polymers (**3**−**5**) reveal that both **1** and **3**−**5** have good thermal stability. The pure phase of compounds **3**, **4**, and **5** is confirmed by XRD

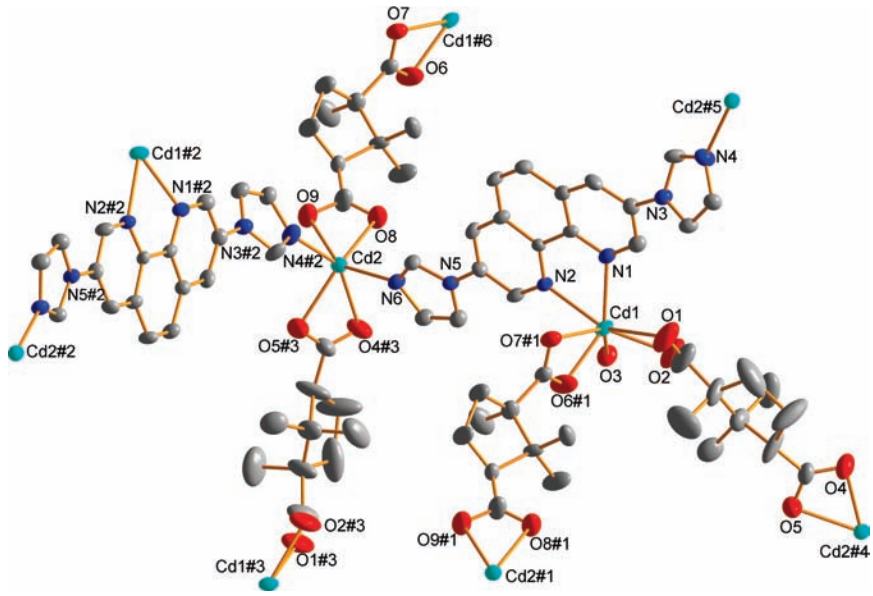

Figure 5. ORTEP drawing of **4** showing 30% probability level ellipsoids (hydrogen atoms are omitted for clarity). Symmetry codes: #1: $-2 + x$, y, $-1 + z$; #2: $1 - x$, $0.5 + y$, $2 - z$; #3: $2 - x$, $0.5 + y$, $1 - z$; #4: $2 - x$, $-0.5 + y$, $1 - z$.

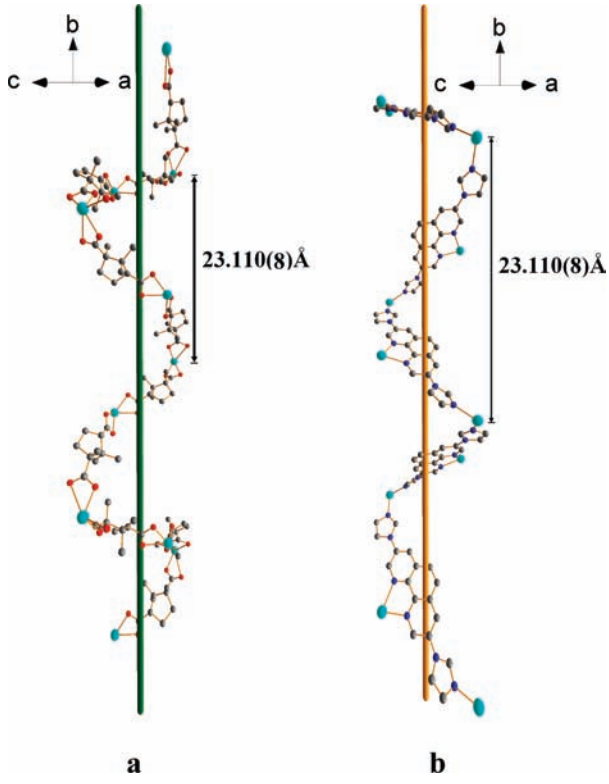

Figure 6. Perspective view of the (a) D-cam/Cd(II)/D-cam and (b) imi/Cd(II)/imi helical chains in **4**.

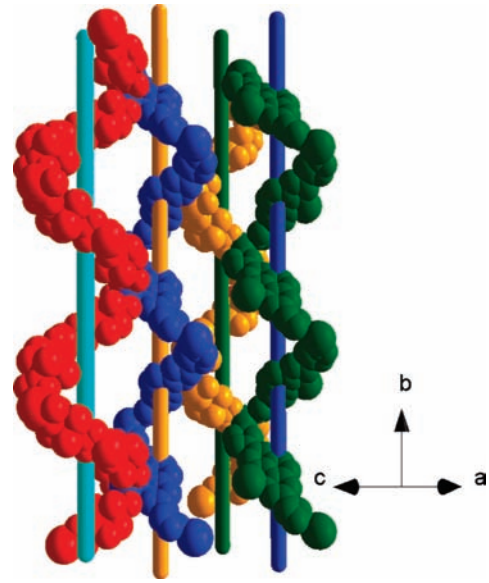

Figure 7. Space-filling view of the 3D helical coordination polymer alternately arranged by D-cam/Cd(II)/D-cam and imi/Cd(II)/imi helical chains in **4**.

patterns (see Figure S1 in the Supporting Information). The TGA curve for **1** shows no weight loss until 618 K and a rapid weight loss process from 619 to 739 K corresponding to a differential thermal peak at 695 K, indicative of the decomposition of compound. All the TGA curves of **3**, **4**, and **5** show two weight loss processes, which are separated by one zero weight loss platform. The first one corresponds to the loss of six lattice water molecules in **3** (7.87% from 293 to 353 K, calculated 7.98%), five lattice water molecules in **5** (7.32% from 293 to 365 K, calculated 7.25%), and one coordination water molecule in **4** (1.85% from 293 to 447 K, calculated 1.89%). The second weight loss process in **3**−**5** is a continuous one corresponding to the decomposition of metal complexes (starting from 617 K in **3**, 641 K in **4**, and 589 K in **5**).

Luminescence Properties. The solid-state fluorescence spectra of 3,8-diimidazol-1,10-phen and its Cd(II) and Zn(II) metal complexes at room temperature are depicted in Figure 10. Compared with phen, in which a fluorescence emission band is observed at $\lambda_{max} = 381$ nm with a shoulder at 364 nm upon excitation at 339 nm,[27] 3,8-diimidazol-1,10-phen exhibits two strong violet emission peaks at 428 and 448

(27) (a) Du, Z. Y.; Li, X. L.; Liu, Q. Y.; Mao, J. G. *Cryst. Growth Des.* **2007**, *7*, 1501. (b) Li, P. Z.; Lu, X. M.; Yang, X. Z. *Inorg. Chim. Acta* **2008**, *361*, 293.

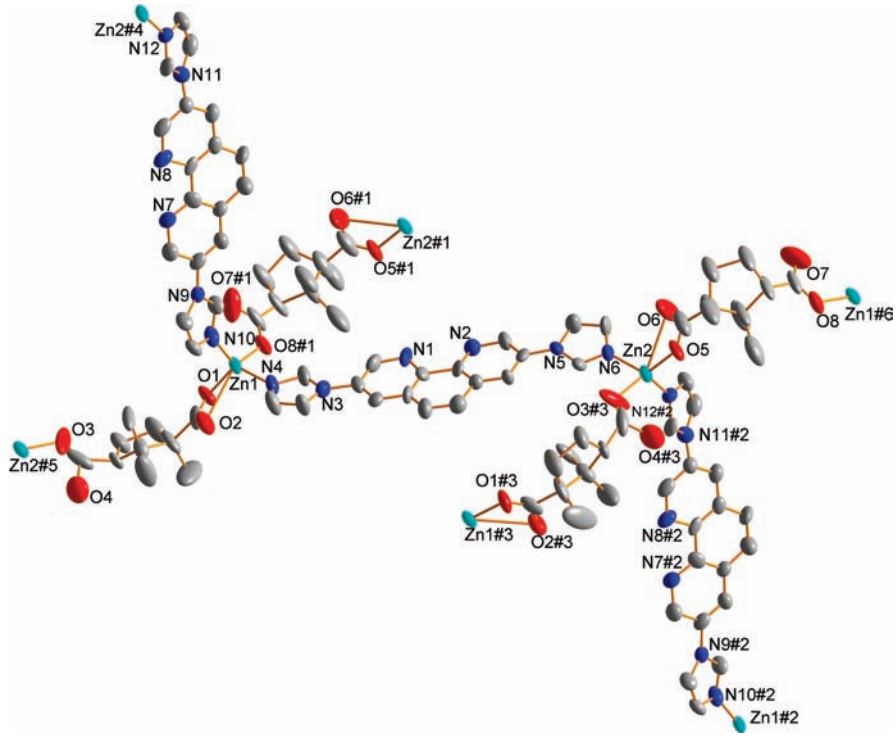

Figure 8. ORTEP drawing of **5** showing 30% probability level ellipsoids (hydrogen atoms are omitted for clarity). Symmetry codes: #1: $2 - x$, $0.5 + y$, $-z$; #2: x, $-1 + y$, $-1 + z$; #3: $1 - x$, $-0.5 + y$, $1 - z$; #4: x, $1 + y$, $1 + z$; #5: $1 - x$, $0.5 + y$, $1 - z$; #6: $2 - x$, $-0.5 + y$, $-z$.

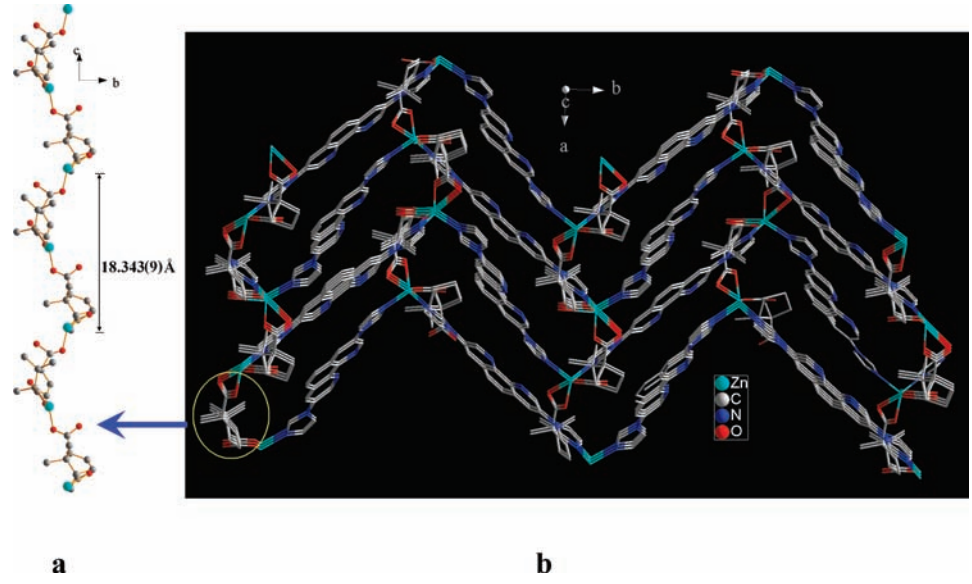

a **b**

Figure 9. View of the (a) D-cam/Zn(II) helical chain and (b) the 3D coordination polymer where the L_b ligands are packed in a zigzag mode in **5**.

nm upon excitation at 395 nm. The several tens of bathochromic shifts for ligand arise from the presence of a large conjugated π-system of the molecule.

After the metal-ion complexation with Zn(II) and Cd(II) centers, blue or green luminescence is observed for **3**−**5**. Complex **3** displays a strong blue fluorescence emission band at 453 nm with the excitation at 394 nm. Complex **4** shows a broad and weaker emission band at 466 nm with the excitation at 400 nm, whereas complex **5** manifests a broad fluorescence emission band at 468 nm with the excitation at 399 nm. The observation of red-shifts in their solid-state fluorescence emission spectra before and after the metal-ion complexation is mainly due to the contribution of 3,8-diimidazol-1,10-phen because the D-cam ligand is fluorescence inactive. The affixation of coordination bonds with the ligand in different molecular conformations and hence the increase of the rigidity of the structures and the participancy of d^{10} metal ions are suggested to be responsible for this bathochromic effect.

Second Harmonic Generation Measurements. Considering that complexes **3**−**5** crystallize in the chiral space groups, nonlinear optical properties of these d^{10} metal complexes in this work are investigated. According to the principles proposed by Kurtz and Perry,[28] the strength of

(28) Kurtz, S. K.; Perry, T. T. *J. Appl. Phys.* **1968**, *39*, 3798.

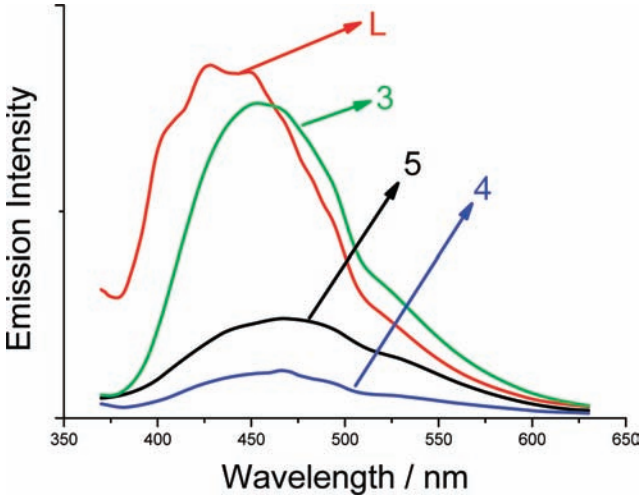

Figure 10. Solid-state fluorescence emission spectra of 3,8-diimidazol-1,10-phen, **3**, **4**, and **5** at room temperature.

the second harmonic generation (SHG) efficiency of the complexes **3**, **4**, and **5** was tested by measuring the microcrystalline powder samples. Preliminary experimental results show that **3**, **4**, and **5** are SHG-active and the SHG efficiency is approximately 0.5, 0.5, and 0.2 times that of urea, respectively, which is consistent with their noncentric frameworks.

Conclusions

In summary, we have described the crystal structures of 3,8-diimidazol-1,10-phen and its dihydrate prepared from the carbon−nitrogen bond cross-coupling reaction from 3,8-dibromo-1,10-phen and imidazole with different molecular conformations (cis/trans in **1** and cis/cis **2**), and two cadmium(II) and one zinc(II) homochiral coordination polymers involving an auxiliary chiral camphorate ligand, formulated as $[Cd_2(D\text{-cam})_2(L_a)_2]\cdot(H_2O)_6$ (**3**), $[Cd_2(D\text{-cam})_2(L_a)(H_2O)]$ (**4**), and $[Zn_2(D\text{-cam})_2(L_b)_2]\cdot(H_2O)_5$ (**5**). 3,8-Diimidazol-1,10-phen ligand in the resulting metal complexes shows different molecular conformations (trans/trans in **3** and **4**, and cis/trans in **5**), versatile coordination modes (the coordination number varying from 2, 3 to 4 in complexes **5**, **3**, and **4**) and architectures (phen/Cd^{II}/imi and imi/Cd^{II}/imi helical chains in **3** and **4**, and zigzag chains in **5**). In complexes **3**−**5**, two D-cam ligands adopt the cis conformation around the metal centers relative to two 3,8-diimidazol-1,10-phen ligands (or one 3,8-diimidazol-1,10-phen ligand and one coordination water molecule around the Cd1 center in **4**), forming a homochiral 2D coordination polymer in the case of **3** and two homochiral 3D coordination polymers in the cases of **4** and **5**. Alteration of the radii of Cd(II) and Zn(II) cations and the molar ratios of four starting materials in the process of metal-ion complexation is suggested to contribute to forming different networks of **3**−**5**. DFT computations have been used to compare the energy differences between the single-crystal and the energy-minimized structures in different conformations (trans/trans, trans/cis, and cis/cis) between the imidazole rings and their bonded phen ring. Moreover, spectral, nonlinear optical, and thermal properties for related compounds before and after the metal-ion complexation have been investigated.

Acknowledgment. W.H. acknowledges the Major State Basic Research Development Programs (2007CB925101 and 2006CB806104), the National Natural Science Foundation of China (20871065 and 20721002), and the Scientific Research Foundation for the Returned Overseas Chinese Scholars, State Education Ministry for financial aid.

Supporting Information Available: Crystallographic information files (CIFs) for compounds **1**−**5**; XRD patterns of compounds **3**−**5** (PDF)..In addition, CCDC reference nos. 714495−714499 contain the supplementary crystallographic data of all five structures. The data can also be obtained free of charge at www.ccdc.cam.ac.uk/conts/retrieving.html [or from the Cambridge Crystallographic Data Centre, 12, Union Road, Cambridge CB2 1EZ, UK; Fax: (Internet.) +44−1223/336−033; E-mail: deposit@ccdc.cam.ac.uk]. This material is available free of charge via the Internet at http://pubs.acs.org.

IC802445Q